

# Wind-tunnel and field investigation of the effect of local wind direction on speed-up over hills

William David Lubitz<sup>a,\*</sup>, Bruce R. White<sup>b</sup>

<sup>a</sup>*School of Engineering, University of Guelph, Guelph, Ont., Canada N1G 2W1*

<sup>b</sup>*Department of Mechanical and Aeronautical Engineering, University of California, Davis, One Shields Ave., Davis, CA 95616 5294, USA*

Received 2 December 2005; received in revised form 3 September 2006; accepted 12 September 2006  
Available online 25 October 2006

---

## Abstract

Measurements of flow past simulated sinusoidal hills were taken in an atmospheric boundary layer wind tunnel (ABLWT) that modeled typical full-scale complex terrain for many wind turbine locations in the Altamont Pass, California, USA. Velocity profiles and speed-up factors for several model hills were determined. All hills modeled had the same height and sinusoidal cross-section, and length-to-width aspect ratios of infinity, four and one. Each of the three models was tested with approach wind directions from 0° to 90°, in 15° increments. It was observed that speed-up can vary significantly depending on the approaching wind direction. The effect of wind direction on speed-up was also investigated using field data from a site in the Altamont Pass. Average speed-up factor was found to vary significantly at the site in time, and as a function of atmospheric stability.

© 2006 Elsevier Ltd. All rights reserved.

*Keywords:* Wind tunnel; Complex terrain; Speed-up; Wind direction; Hill; Altamont Pass

---

## 1. Background

Much work has been done developing simplified models for predicting wind “speed-up” in complex terrain. Speed-up is the increase of near-surface wind speed above a hill as compared to the wind over a flat surface at the same height above the surface.

---

\*Corresponding author. Tel.: +1 519 824 4120x54387; fax: +1 519 836 0227.

E-mail addresses: [wlubitz@uoguelph.ca](mailto:wlubitz@uoguelph.ca) (W.D. Lubitz), [brwhite@ucdavis.edu](mailto:brwhite@ucdavis.edu) (B.R. White).

Non-dimensionally it is expressed as the fractional speed-up ratio:

$$\Delta S = \frac{U(z) - U_0(z)}{U_0(z)}, \quad (1)$$

where  $U$  is the wind speed at a height  $z$  above the hill, and  $U_0$  is the upstream speed of the hill at the same height. It is assumed that the approach to the hill is a flat surface with the same surface roughness as the hill.

Jackson and Hunt (1975) developed an analytical method to predict speed-up over a two-dimensional, smooth hill without flow separation, which was subsequently improved (Hunt et al., 1988). Jackson also examined the implications of this approach, as well as wind-tunnel and numerical methods, for evaluating potential wind turbine sites (Jackson, 1979). Other researchers have made extensions to the Jackson and Hunt methods. For example, Mason and Sykes (1979) extended the method of Jackson and Hunt to a single three-dimensional axisymmetric hill. The body of work based on Jackson and Hunt remains essentially the only satisfactory analytical method of estimating speed-up over hills.

Kaimal and Finnigan (1994) report that the results of Jackson and Hunt were used to formulate a set of widely used simple guidelines to estimate the maximum speed-up  $\Delta S_{\max}$  expected to be observed over simple topographic features with slopes low enough to not experience flow separation (i.e., geometric divergence angles of less than 15–18° from the mean flow direction)

$$\Delta S_{\max} \approx 1.6h/L_1 \quad \text{for axisymmetric hills,} \quad (2a)$$

$$\Delta S_{\max} \approx 2.0h/L_1 \quad \text{for 2D ridges.} \quad (2b)$$

Here  $L_1$  is the horizontal distance from the hill peak of height  $h$  to the point on the slope at height  $h/2$  (the “half-height” of the hill). This set of equations is generally considered to be accurate to  $\pm 15\%$ .

There have been numerous experimental studies that investigated speed-up over two-dimensional hills. Gong and Ibbetson (1989) performed wind-tunnel tests on a two-dimensional ridge and a circular hill, both with cosine squared cross-sections. Miller and Davenport (1998) conducted wind-tunnel tests of two-dimensional model hills, and presented tables of speed-up values for different approach slopes and upwind conditions. Weng et al. (2000) also present guidelines for two-dimensional hills, based on hill geometry and surface roughness; additionally, they report the results of several wind-tunnel tests. Taylor (1998) conducted numerical simulations of flow over low and moderate slope hills, and presented an equation to predict speed-up based on hill parameters. Kim et al. (1997) experimentally and numerically investigated the effects of hill slope on speed-up over two-dimensional hills of sinusoidal cross-section. In numerical simulations and field studies of actual hills, Kim et al. (2000) observed that the flow field over a hill was affected by the presence of other hills nearby, and that these hills must be included for accurate results.

Further complicating matters, flow separation occurs in the lee of steep hills (Jackson, 1979). Finnigan (1988) compiled separation data from multiple field and wind tunnel studies. Separation did not occur when maximum slopes were less than 0.27 (15°), always occurred when maximum slope was at least 0.32 (18°), and was intermittent when slopes were between these values. For two-dimensional, sinusoidal hills, Kim et al. (1997) and Miller and Davenport (1998) both used the criterion that separation occurred for hills with

slopes exceeding 0.4 (22°). Once separation occurs, accurate speed-up predictions became significantly more difficult.

There have been several empirical speed-up prediction algorithms published that provide formulae or look-up tables to predict speed-up for arbitrary hills. The ESDU (1990) wind speed prediction algorithm incorporates a correction factor for sites on or near two-dimensional escarpments that was derived from wind-tunnel data and field work of Bowen and Lindley (1977) and the numerical studies of Deaves (1980). The correction factor (called  $K_L$ ) is presented in a series of lookup graphs for different escarpment slopes.

Taylor and Lee (1984) present a simple speed-up prediction algorithm (the “original Guidelines”) that allowed the prediction of  $\Delta S$  above a hilltop at various heights above ground  $z$ . Speed-up can be predicted over a hill that is either isolated, or located among regularly repeating hills, as would occur in rolling terrain. The original Guidelines predict a maximum speed-up  $\Delta S_{\max}$  based on hill height  $h$  and the hill half-length  $L_1$ . It is then assumed that  $\Delta S$  varies exponentially with height  $z$

$$\Delta S_{\max} = Bh/L_1, \quad (3a)$$

$$\Delta S = \Delta S_{\max} \exp(-Az/L_1), \quad (3b)$$

where  $A$  and  $B$  are constants that depend on the type of hill and surrounding terrain. The original Guidelines can be applied in cases of moderate to high wind speeds on hills with a maximum slope  $< 0.3$ ,  $L_1/z_0 > 100$  and  $L_1 < 2$  km (Taylor and Lee, 1984).

Weng et al. (2000) refined the original Guidelines using a series of numerical simulations, including some non-linear, and based on the results proposed a set of “new Guidelines.” The new Guidelines allow for the variation of surface roughness  $z_0$ , and the prediction of speed-up at the top of steeper hills with slopes up to about 0.5.

There have been minimal laboratory investigations of speed-up over three-dimensional hills that have different horizontal length and width (i.e., aspect ratio not equal to one) in addition to height. Lemelin et al. (1988), hereafter referred to as LSD, used a series of numerical simulations with the MS3DJH/3R model to derive a set of speedup prediction formulae to predict speedup anywhere above an elliptic paraboloid hill defined by three length scales: in the direction of the approach wind  $L_1$ , perpendicular to the approach wind  $L_2$  and peak height  $h$ . This model was derived for low to moderate slopes (simulations were done at  $h/L_1 = 0.28$ ) and  $150 \leq L_1/z_0 \leq 100,000$ . Given that the LSD method was intended for incorporation into building codes, and was intentionally kept relatively simple, it nonetheless appears to be unique in that it includes the hill aspect ratio. However, the LSD equations do not predict the observed negative speed-up values that occur at the base of very steep hills, and like most methods, only consider winds at right angles to the hill.

### 1.1. Wind direction

No comprehensive results could be found which quantify speed-up as a function of the approach direction of the wind. If wind direction is addressed at all, most empirical speed-up prediction methods use simple correction factors to account for the wind direction. Baker (1985) conducted model and full-scale tests of 27° (0.51) slope railroad embankments, and found the speed-up algorithm outlined by ESDU (1990) worked well when the flow was perpendicular to the embankment. Baker noted that with non-orthogonal winds, only the velocity component normal to the embankment is accelerated,

and derived an equation to modify the ESDU “ $K_L$ ” factor ( $K_L = 1 + \Delta S$ ) to include wind direction. Expressed in terms of speed-up factor

$$\Delta S(\theta) = ((1 + \Delta S_0)^2 \cos^2 \theta + \sin^2 \theta)^{1/2} - 1, \quad (4)$$

where  $\theta$  is the angle of the wind direction off perpendicular and  $\Delta S_0 = \Delta S(\theta = 0^\circ)$  is the  $\Delta S$  that would be estimated with a wind direction perpendicular to the embankment.

A United States Federal Aviation Administration (FAA) (1988) model of speed-up for a two-dimensional ridge is similar to the original Guidelines, except that the model adds a wind direction correction in which the horizontal length scale of the ridge is measured across the ridge in the same direction as the wind is blowing. The half-length of the hill is taken in the direction of the approach wind by using the relation  $L_0 = L_1 / \cos \theta$ , with  $L_1$  and  $L_0$  being the half-lengths of the hill in the direction perpendicular to the ridgeline and in the direction aligned with the wind, respectively, while  $\theta$  is the angle of the approach wind direction relative to normal to the ridgeline. (i.e.  $\theta = 0^\circ$  is a wind normal to the ridge,  $\theta = 90^\circ$  is a wind parallel to the ridgeline.) This method is straightforward to implement, and the wind direction modification would appear to result in conservative (i.e., relatively high) speed-up estimates at mid-ranges of  $\theta$ .

## 2. Wind-tunnel tests of generalized hills

For speed-up predictions to be applicable to wind energy uses, the wind direction must be factored into the prediction algorithm. Additionally, the algorithm would need to include more than circular and two-dimensional hill shapes. Since little systematic data are available in the literature documenting how speed-up varies based on these parameters, a series of tests of generalized hills were performed in the University of California (US), Davis atmospheric boundary layer wind tunnel (ABLWT) to gain insight into how the wind direction impacts speed-up over a hill.

### 2.1. Test specifications

The UC Davis ABLWT is an open-return type tunnel, shown in Fig. 1. Wind speeds within the tunnel can be varied from 1 to 10 m/s (2–22 mph). A series of spires at the inlet and a 12 m long flow development section is used to generate a mature turbulent boundary layer at the test section. Diverging walls and an adjustable ceiling in the development section maintain a zero-pressure-gradient flow. Roughness elements are placed on the floor of this section to generate the appropriate boundary-layer height in the test section. The test section is 3.7 m long, 1.7 m high and 1.2 m wide. A three-dimensional traversing system mounted to the ceiling of the test section allows for precise placement of a sensor at any point within the test section. Small 1 mW lasers are mounted on the traverser to sight vertical height and horizontal position within  $\pm 0.5$  mm.

Mean velocity and turbulence intensity are measured using single wire, end flow hotwires (TSI Model 1210-20). The hotwire is supported on the end of a straight 50 cm probe, which in turn is secured to the internal three-dimensional traversing system in the test section of the ABLWT. The hotwire sensor element is electrically connected via a 10 m shielded tri-axial cable to a constant temperature thermal-anemometry unit with a signal conditioner, TSI Model IFA 100. The analog signal from the signal conditioner is passed to a 12-bit analog to digital (A/D) converter and then to a computer for analysis and data

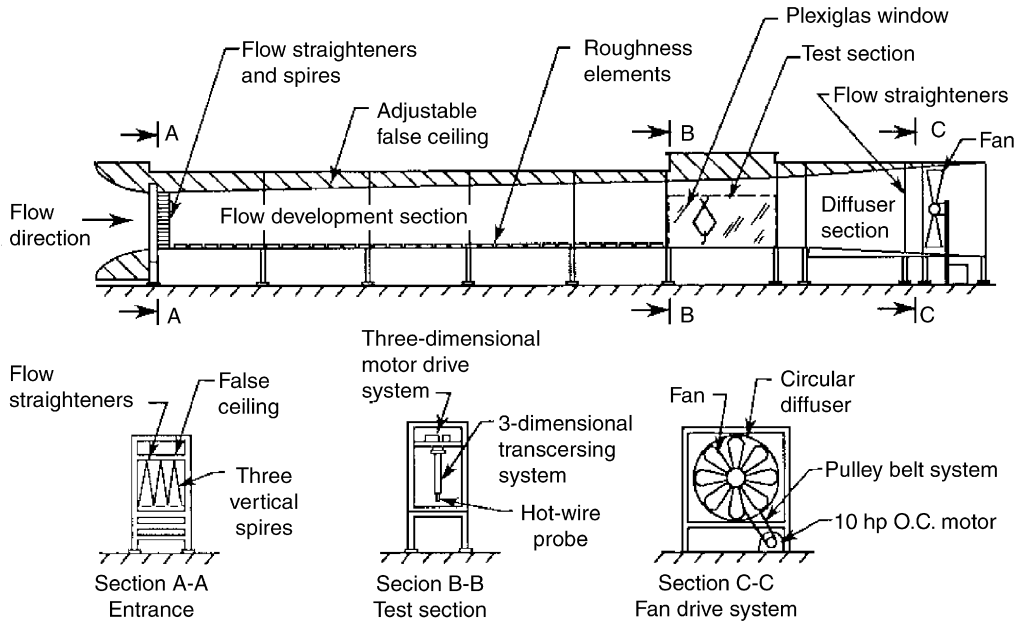


Fig. 1. Schematic of UC Davis atmospheric boundary layer wind tunnel.

storage by a National Instruments LabView program. Thermal anemometry has been widely used in measuring turbulent flow for its ability to sample flow velocity at frequencies up to or exceeding 1000 Hz. Typically, hotwire measurements made close to the surface have an uncertainty of less than  $\pm 5\%$  of the true values. A mechanical height probe and the laser-spotting system were used to position the hot-wire. Hot-wire measurements were taken at 1000 Hz for 90 s.

A power law exponent of  $\alpha = 0.19$  was achieved by systematically arranging an arrayed pattern of  $8.3 \times 19.7 \times 3.8$  cm blocks in the upwind half of the development section, and  $8.9 \times 14.6 \times 1.9$  cm blocks in the downwind half of the development section. Artificial grass was used in the test section (mean height of 3 mm) and extended upwind and under the blocks. Additionally, the first three rows of blocks upwind of the test section were replaced with smaller blocks (Fig. 2) to create a smooth flow transition from the roughness elements to the hill model. Fig. 3 shows typical mean velocity profiles produced by this arrangement.

## 2.2. Hill models

Three different hill models were manufactured from polystyrene foam. All of the hills had a cosine cross-section and a height of  $h = 38$  mm. An axisymmetric hill with a circular base was produced by revolving the cosine cross-section. An elliptical hill was made by stretching the circular hill so that the resulting elliptical footprint had a base length four times longer than the base width. A semi-infinite (“two-dimensional”) hill model also was constructed with a cosine cross-section. Model surface roughness was maintained on the circular and elliptical hills by reproducing the topography using 2.5 mm steps, while the two-dimensional model was covered in artificial grass. The equation of the height of the



Fig. 2. Roughness element arrangement used in ABLWT development section for generalized hill tests. Also visible is the two-dimensional hill model at  $\theta = 30^\circ$  and the measurement probe support with sighting laser and height probe installed.

surface  $z(x,y)$  of these hills is

$$z = \frac{h}{2} + \frac{h}{2} \cos\left(\frac{\pi}{2L_1}(x^2 + A^2y^2)^{1/2}\right), \quad (5)$$

where  $x$  and  $y$  are the horizontal distances from the hill peak.  $L_1$  and  $L_2$  are the half-lengths of the hill in the  $x$  and  $y$  directions. (The half-length is the distance from the peak to the

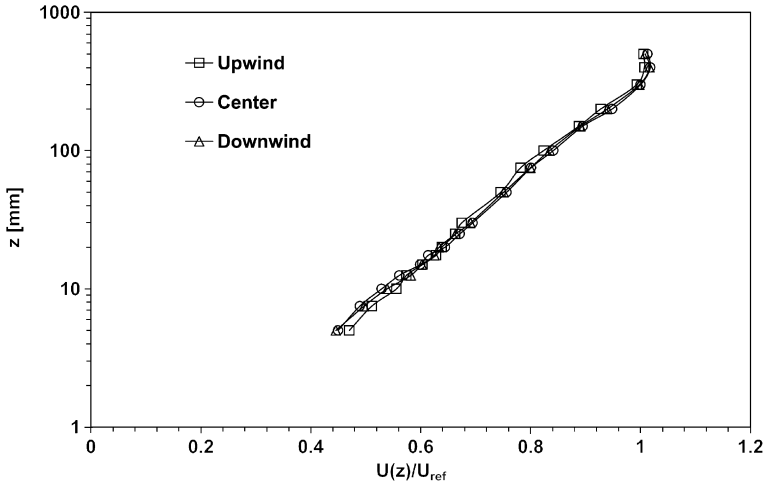


Fig. 3. Non-dimensionalized velocity profiles in empty UC Davis atmospheric boundary layer wind tunnel test section with artificial grass covering floor at three locations: at center, and 68 cm upwind and downwind of center.

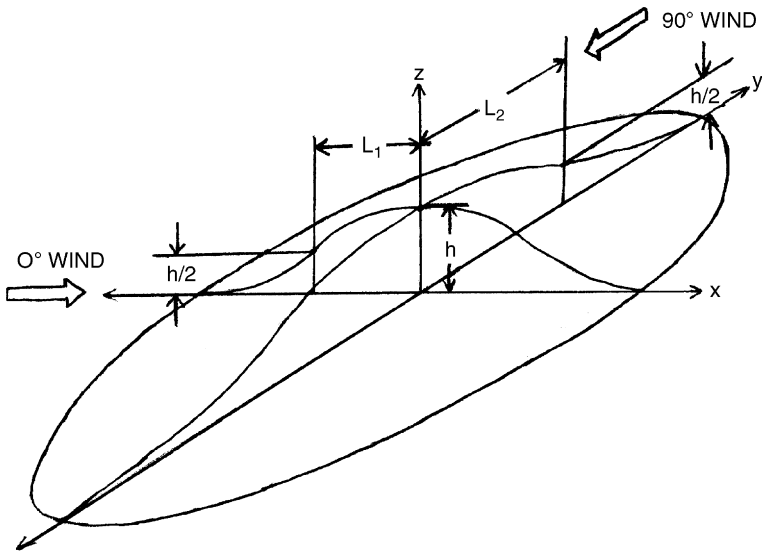


Fig. 4. Schematic diagram of the hill models.

point on the slope where  $z = h/2$ ). The aspect ratio of the hill is  $A = L_2/L_1$ . For the circular, elliptical and two-dimensional models,  $A = 1.0, 4.0$  and  $0$ , respectively. All the models had a primary half-length  $L_1$  of 71.5 mm. Fig. 4 shows a schematic of the hill geometry.

### 2.3. Model roughness

The model surface must be sufficiently rough to maintain a turbulent flow over the model surface. According to Snyder (1981), this means that the roughness Reynolds

number must be greater than about 2.5. Practically, this means that the model must not be “aerodynamically smooth”. Model roughness can be provided by coating or covering the surface in a suitable material. Previous investigators of speed-up over two-dimensional hills have used studded rubber sheets (Gong and Ibbetson, 1989), artificial grass (Kim et al., 1997), uniformly spread sand (Baker et al., 1985) and textured wall paper (Carpenter and Locke, 1999).

Roughness also can be achieved by using “steps” or “terraces.” This latter type of roughness can be a by-product of model construction: if the terrain is carved from a large block of material using mapped contours to guide the cutting tool, the result is a “stepped” model where the edge of each step follows one of the mapped contour lines. The maximum step size will depend on the scale of the features modeled, since larger steps cause a greater departure from geometric similarity. Derickson and Peterka (2004) tested a 1:4000 scale model of complex terrain of Lantau Island, Hong Kong, in an ABLWT, using a model with 3 mm steps. The space between the steps was then carefully filled with plaster to make a “smoothed” model, and the test was run again. Little difference was observed in the resulting near-surface velocity profiles measured at several points on the model. If the steps become too large, however, they start to interfere with the properties of the flow: Lindley et al. (1981) modeled Gebbies Pass, New Zealand at 1:4000 scale in both stepped and “smooth” configurations, and found the stepped model performed very poorly. This may be attributable to the large step size of 1 cm, and the fact that the range between the highest and lowest points on the model encompassed only 11 steps. Although generally low, the effect of model roughness is most pronounced at and downstream of separation points on the model since the exact location of a separation point is a strong function of perturbations in the local model geometry and generally unsteady in time. Miller and Davenport (1998) performed ABLWT tests on two-dimensional sinusoidal hill models with maximum slopes of 0.5 (27°), steep enough to expect lee side flow separation, and reported velocities corresponding to speed-up factors as high as 1.4 at the surface on the hill peak, although the speed-up decreased rapidly with height and was minimal above  $z/h \approx 0.5$ .

The circular and elliptical hill models in this study were fabricated with 2.5 mm steps. The two-dimensional ridge was covered in artificial grass to ensure a consistent surface roughness regardless of orientation in the wind tunnel. For all three hills, artificial grass covered the entire floor in the test section. Previous experiments showed that if the test section floor was left as an untreated bare plywood surface, an internal boundary layer formed in the test section, causing unacceptable variation in velocity measurements with test section position.

#### 2.4. Uncertainty of measured speed-up values

There are two main sources of error in the reported speed-up values: errors due to the position of the probe being slightly off from its correct measurement location, and errors due to the measurement process itself.

To quantify measurement uncertainty, or repeatability, trial experiments were performed in the ABLWT repeatedly measuring mean velocity at the same point. Two measurement points were used to cover the range of flows encountered during the experiments: in the center of the tunnel at reference height (high speed flow with 5% turbulence intensity) and in the near-wake of a large block (low speed flow with 30%

turbulence intensity). The standard deviation of measured mean velocity was 0.17% and 0.46%, respectively at these points, suggesting good repeatability.

For these tests, positioning uncertainty is considered to be  $\pm 1$  mm vertically, and  $\pm 0.5$  mm horizontally. This is due mainly to the difficulty of precisely fixing the ground level relative to the artificial grass surface. Positioning errors will produce the greatest uncertainties in wind speed measurement near the surface, where the spatial variation of the flow field is greatest. It is also noted that the stepped nature of the models means that the model geometry may differ from the “true” geometry by up to 1 mm vertically. Near the surface, the level of uncertainty due to positioning error is greater than that resulting from the measurement process itself.

Since  $\Delta S$  is a normalized difference of two wind speeds, the uncertainty of  $\Delta S$  is greater than the uncertainty of the individual measured wind speeds. Uncertainty in  $\Delta S$  varies greatly depending on the location of the measurement, and the local value of  $\partial U/\partial z$ . In high shear at the lowest measurement level of 5 mm above the surface,  $\Delta S$  uncertainty of up to 0.4 is possible, based on measured spatial variations in velocity. For all other measurement locations, worst-case uncertainty in  $\Delta S$  is 0.1, and most measurement locations will have lower actual uncertainty than these values.

Practically, the speed-up results for the two-dimensional hill with a  $90^\circ$  wind (Table 1) give a good indication of the level of uncertainty in the speed-up results. Since the hill is aligned with the wind and extends beyond the test section both upwind and downwind, all of the speed-ups observed should be zero. The average mean absolute speed-up factor error for all three locations and all nine measurement heights was 0.027; the greatest error in the measurements was  $\Delta S = -0.067$  near the surface at the hill base.

An additional source of potential error is that the wind tunnel has a finite width of 1.17 m (46 in). Previous measurements in the ABLWT have shown that a boundary layer approximately 8 cm thick at the test section exists adjacent to each side wall, precluding measurements near the wall. Additionally, the wind velocity adjacent to the wall must be tangent to the wall, meaning that tunnel walls affect the local flow direction (and by extension, the velocity distribution) for a distance somewhat greater than 8 cm in from either wall. For this study, the majority of measurements were made near the tunnel centerline, and none were less than 17 cm from a side wall.

Table 1  
Measured speed-up factors for the two-dimensional hill with wind from  $90^\circ$

$z/L$	Face $x/L$		Base
	Top		
	0	-1	-2
0.07	-0.013	-0.043	-0.067
0.10	0.014	-0.027	-0.041
0.14	0.024	-0.024	-0.033
0.17	0.031	-0.018	-0.021
0.21	0.047	-0.009	-0.014
0.28	0.035	0.004	-0.014
0.42	0.053	0.011	0.005
0.70	0.047	0.017	0.010
1.05	0.063	0.027	0.011

## 2.5. Test specifications

Measurements were taken at five similar points on both the two-dimensional and elliptical hills: at the base and half-height on both windward and leeward slopes, and at the hilltop. Profiles also were taken at both half-height points along the long axis of the elliptical hill. Measurements were taken at  $z = 5, 7.5, 10, 12.5, 15, 20, 30, 50$  and  $75$  mm above each point, giving a range of  $z/h$  between 0.13 and 1.97. The elliptical and two-dimensional models were rotated and individually tested in the ABLWT to simulate wind from  $0^\circ, 15^\circ, 30^\circ, 45^\circ, 60^\circ, 75^\circ$  and  $90^\circ$  relative to the short axis of the hill. Since the models were symmetric, this was sufficient to characterize the velocity profile for wind from  $+90^\circ$  to  $-90^\circ$  at  $15^\circ$  intervals. Similar measurements were taken to characterize the same points on the circular hill. As the two-dimensional hill model was rotated, additional sections were added to the model so that it extended to flush interfaces with both side walls of the test section at angles up to  $75^\circ$ . For the  $90^\circ$  test, the two-dimensional hill model was terminated at the downwind edge of the test section and 2 m upwind into the development section by smoothly bringing the artificial grass surface down to floor level over approximately 0.5 m.

Additionally, for each model and wind direction, profiles of mean velocity and turbulence intensity were taken upwind of the hill location for all directions up to  $60^\circ$ . This was not possible for the  $75^\circ$  and  $90^\circ$  directions, where portions of the hill models themselves were effectively upwind. For these directions, an average of the mean velocity profiles for the other directions was used to calculate speed-up factors. Since the profiles showed minimal variation, this was not considered to have introduced significant error.

## 2.6. Two-dimensional ridge and three-dimensional circular hill

Most previous wind-tunnel studies concentrated on two hill configurations: two-dimensional ridges with the wind blowing perpendicularly across the ridge, and three-dimensional axisymmetric hills with a circular “footprint”. Both of these configurations were tested in the UC Davis ABLWT. Results were reasonably consistent with other studies. Table 2 summarizes the characteristics and maximum speed-up results observed at the hill peak in several previous studies. The greatest speed-up occurs very near the surface in all of these studies, either at the lowest measured point (designated as “surface” in the table) or only a few measurement points above the surface. Interestingly, Eqs. (2a) and (2b) are found to overpredict the maximum speed-up  $\Delta S_{\max}$ , generally by more than 15%, for every data set except Gong and Ibbetson’s (1989), which show very good agreement between measurements and Eqs. (2a) and (2b).

## 2.7. Test results

Generally, the range of speed-up factors observed for the two-dimensional hill was somewhat greater than the range observed over the elliptical hill. For the top of the two-dimensional hill (Fig. 5), speed-up factors at angles near  $0^\circ$  were the highest ( $\Delta S = 0.68, 0.72$ ) at the lowest measurement point 5 mm above the surface, and decreased as height above the surface increased ( $\Delta S = 0.50$  at  $z = 12.5$  mm). At angles greater than  $45^\circ$  the variation in  $\Delta S$  decreases, as the component of the wind parallel to the slope increases, until at  $90^\circ$ ,  $\Delta S < 0.06$  for all of the measurement points and heights. Speed-up at the top of

Table 2  
Summary of several wind-tunnel tests of two-dimensional and three-dimensional axisymmetric hills

	Two-dimensional ridge						4:1 elliptical hill	Three-dimensional axisymmetric hill		
	H3 EPA 1981 (Weng et al., 2000)	Miller and Davenport (1998)	UC Davis	H5 EPA 1981 (Weng et al., 2000)	Gong and Ibbetson (1989)	H8 EPA 1981 (Weng et al., 2000)	UC Davis	Ohba et al., 2002	UC Davis	Gong and Ibbetson (1989)
$H$ [mm]	117	96.5	38	117	31	117	38	100	38	35
$L_1$ [mm]	175.5	152.5	71.5	292.5	100	468	71.5	~200	71.5	100
$H/L_1$	0.67	0.63	0.53	0.40	0.31	0.25	0.53	~0.5	0.53	0.35
$Z_0$ [mm]	0.16	0.16	0.20	0.16	0.17	0.16	0.20	N/A	0.20	0.17
$U^*/U_\infty$	0.046	N/A	0.019	0.046	0.055	0.046	0.019	N/A	0.019	0.055
Hill profile	Parametric	Cosine	Cosine	Parametric	$\text{Cos}^2$	Parametric	Cosine	Custom	Cosine	$\text{Cos}^2$
Max slope [rise/run]	0.49	0.5	0.42	0.29	0.25	0.19	0.42	~0.5	0.42	0.29
Observed $\Delta S_{\max}$	1.08	~0.8	0.68	0.70	0.61	0.35	0.74	0.43	0.69	0.56
Height of observed $\Delta S_{\max}$ [z/h]	Surface	0.1	Surface	Surface	0.15	0.15	Surface	Surface	0.2	0.17
Predicted $\Delta S_{\max}$ [Eqs. (2)]	1.33	1.27	1.06	0.80	0.62	0.50	1.06	0.80	0.85	0.56

EPA RUSHIL data from Ref. (Weng et al., 2000). Surface roughness ( $z_0$ ) is for approach wind profile. Values for height and value of observed  $\Delta S_{\max}$  is taken from experimental data, with a height of “surface” indicating  $\Delta S_{\max}$  occurred at the lowest measured point in the profile. “UC Davis” indicates data from this study. “Elliptical Hill” data is for wind direction perpendicular to the long axis of the hill. N/A indicates data was neither given nor derivable from published results.

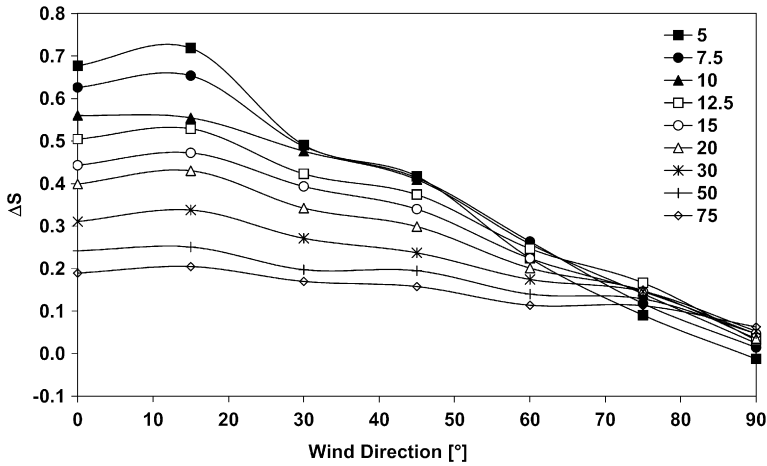


Fig. 5. Speed-up factor versus wind direction for two-dimensional hill at hilltop. Heights from 5 to 75 mm above the surface are plotted. Wind from 0° is perpendicular to ridgeline. Wind from 90° is parallel to ridgeline.

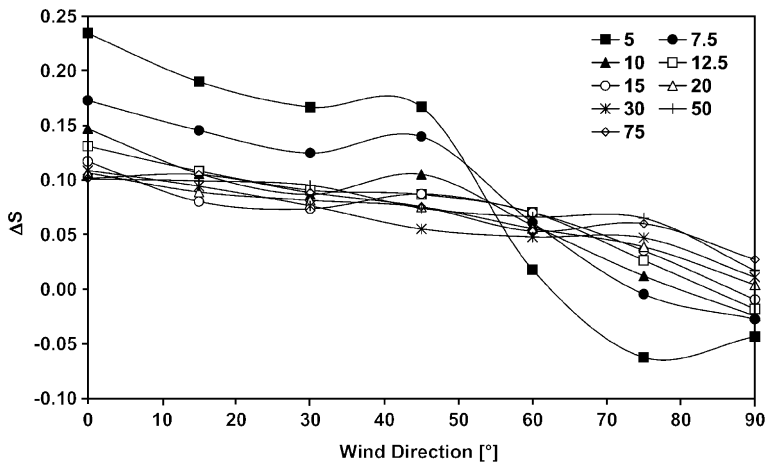


Fig. 6. Speed-up factor versus wind direction for two-dimensional hill on midpoint of hill face. Heights from 5 to 75 mm above the surface are plotted. Wind from 0° is perpendicular to ridgeline. Wind from 90° is parallel to ridgeline.

the elliptical hill (Fig. 8) was similar to the two-dimensional hill for low values of  $\theta$ . As  $\theta$  approached 90°, values of  $\Delta S$  above the elliptical hill top trended to intermediate values typical of a lower sloped hill, instead of to zero as in the case of the two-dimensional hill.

On the slope face ( $x/L_1 = -1$ ) of the two-dimensional hill (Fig. 6),  $\Delta S$  reached a much lower maximum of 0.24, and showed less variation with either height or direction than at the hilltop. Except for very close to the surface, speed-up at a given height varies roughly linearly from a maximum at  $\theta = 0^\circ$  to  $\Delta S \approx 0$  at  $\theta = 90^\circ$ . Speed-up above the face of the elliptical hill (Fig. 9) was higher at  $\theta = 90^\circ$  than at  $\theta = 0^\circ$ , due to the component of the flow being accelerated laterally around the hill as  $\theta$  approached 90°.

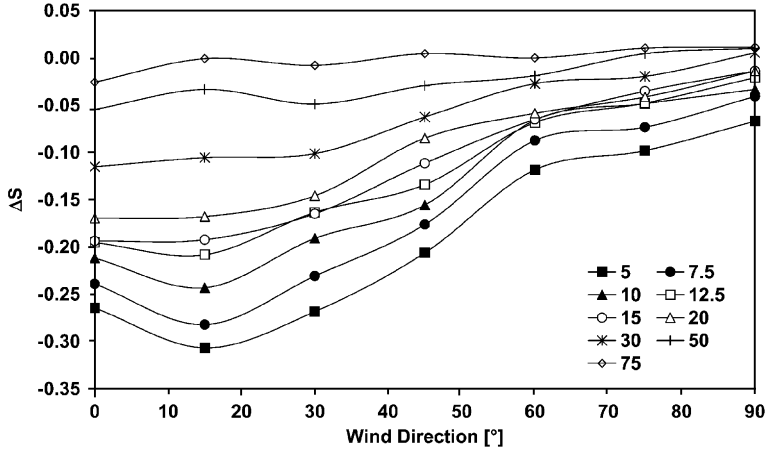


Fig. 7. Speed-up factor versus wind direction for two-dimensional hill at base of hill. Heights from 5 to 75 mm above the surface are plotted. Wind from 0° is perpendicular to ridgeline. Wind from 90° is parallel to ridgeline.

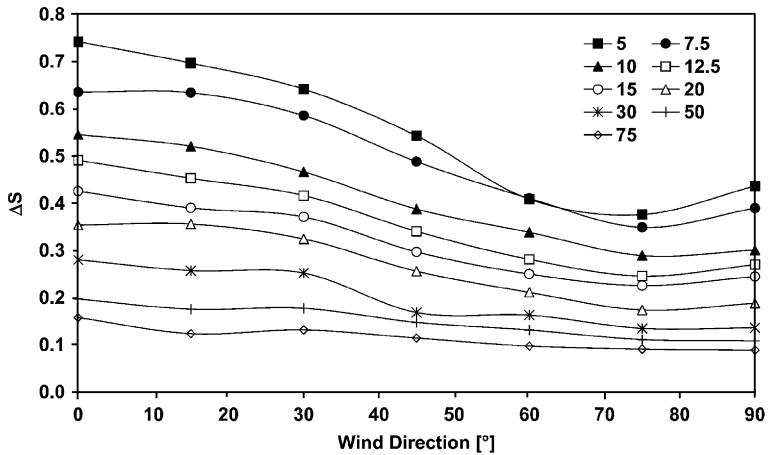


Fig. 8. Speed-up factor versus wind direction for elliptical hill at hilltop. Heights from 5 to 75 mm above the surface are plotted. Wind from 0° is perpendicular to ridgeline. Wind from 90° is parallel to ridgeline.

The hill base area is a region of reduced velocity near the surface at low values of  $\theta$ . For the two-dimensional hill (Fig. 7), the minimum  $\Delta S = -0.27$  occurs at  $z = 5$  mm and  $\theta = 0^\circ$ , and speed-up factors go to zero by  $z/h = 2$ . Similar minimum values of  $\Delta S$  are observed at  $\theta = 0^\circ$  for the elliptical hill (Figs. 10, minimum  $\Delta S = -0.30$ ) and circular hill (Fig. 13, minimum  $\Delta S = -0.25$ ). It is interesting to note that for all three hills,  $\Delta S$  trends uniformly from a minimum at  $\theta = 0^\circ$  to a maximum at  $\theta = 90^\circ$ . While this maximum is approximately zero for the two-dimensional hill, it is higher for the elliptical hill (maximum  $\Delta S = 0.14$ ). The overall trend is higher still for the circular hill.

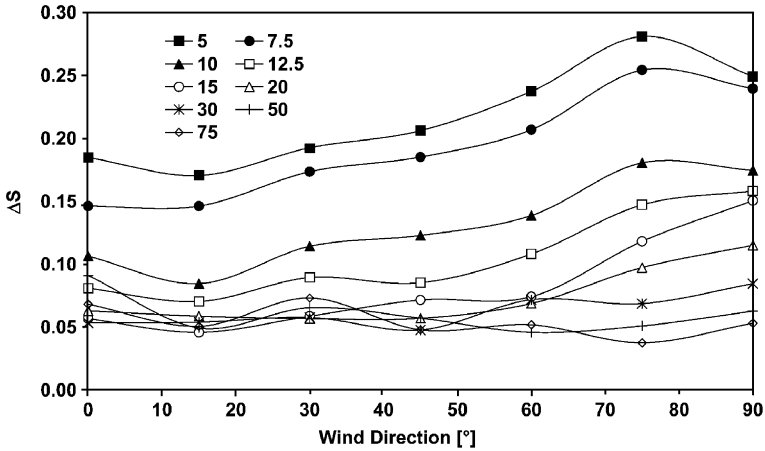


Fig. 9. Speed-up factor versus wind direction for elliptical hill on midpoint of hill face. Heights from 5 to 75 mm above the surface are plotted. Wind from 0° is perpendicular to ridgeline. Wind from 90° is parallel to ridgeline.

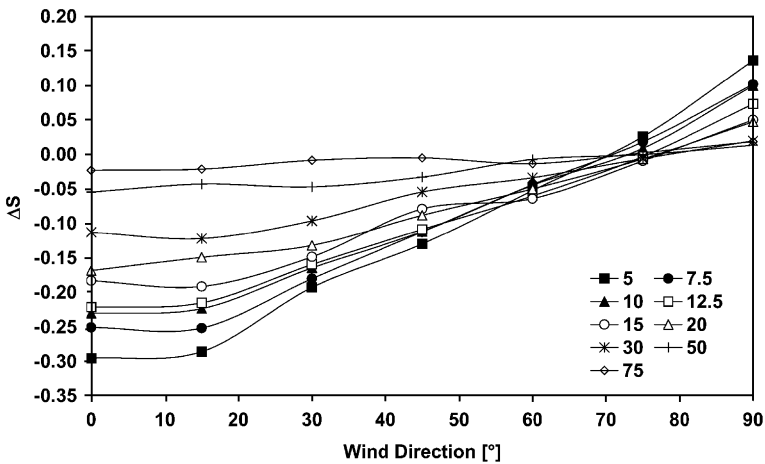


Fig. 10. Speed-up factor versus wind direction for elliptical hill at base of hill. Heights from 5 to 75 mm above the surface are plotted. Wind from 0° is perpendicular to ridgeline. Wind from 90° is parallel to ridgeline.

The variation of  $\Delta S$  with  $\theta$  at the hill face measurement point also depends strongly on the hill aspect ratio. For the two-dimensional hill,  $\Delta S$  trends from maximum values at  $\theta = 0^\circ$  to  $\Delta S \approx 0$  at  $\theta = 90^\circ$  (Fig. 6). For the elliptical hill (Fig. 9), the variation of  $\Delta S$  is less pronounced, with  $\Delta S$  slightly lower at  $\theta = 0^\circ$  than at  $\theta = 90^\circ$ . The trend for the circular hill is opposite that of the two-dimensional hill:  $\Delta S$  trends from minimum values at  $\theta = 0^\circ$  to maximum values at  $\theta = 90^\circ$  (Fig. 12).

Some of the variation in  $\Delta S$  for the circular hill base and face points appears to be caused by a “cross flow” phenomenon. As the wind strikes the circular hill, a percentage of air flows up and over the summit (Fig. 11), with the remaining air flowing horizontally

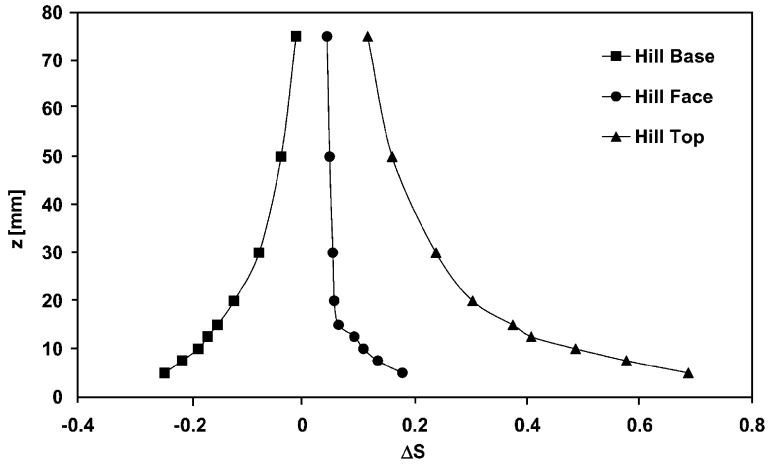


Fig. 11. Speed-up factor versus height for circular hill at top ( $x/L_1 = 0$ ), face ( $x/L_1 = -1$ ) and base ( $x/L_1 = -2$ ).

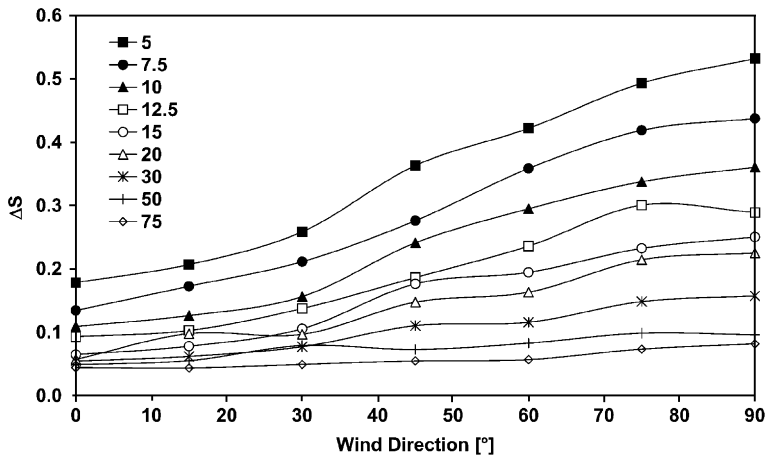


Fig. 12. Speed-up factor versus wind direction for circular hill on midpoint of hill face. Heights from 5 to 75 mm above the surface are plotted. Measurement point is on upwind slope when wind is from  $0^\circ$ . Measurement point is on shoulder of hill when wind is from  $90^\circ$ .

around the sides of the hill. This would cause speed-up factors to be higher around a hill of aspect ratio near unity, whereas this effect would be minimal as the aspect ratio approached 0 or  $\infty$ .

### 2.8. Hill aspect ratio

Combining results from the  $0^\circ$  and  $90^\circ$  wind direction tests of the three hill models, it is possible to observe how  $\Delta S$  changes as a function of the hill aspect ratio  $A$ . Fig. 14 shows the hilltop speed-up profiles for four of the aspect ratios tested. ( $A = 0$  is not plotted as  $\Delta S \approx 0$ ). The speed-up predicted by the LSD method is also plotted.

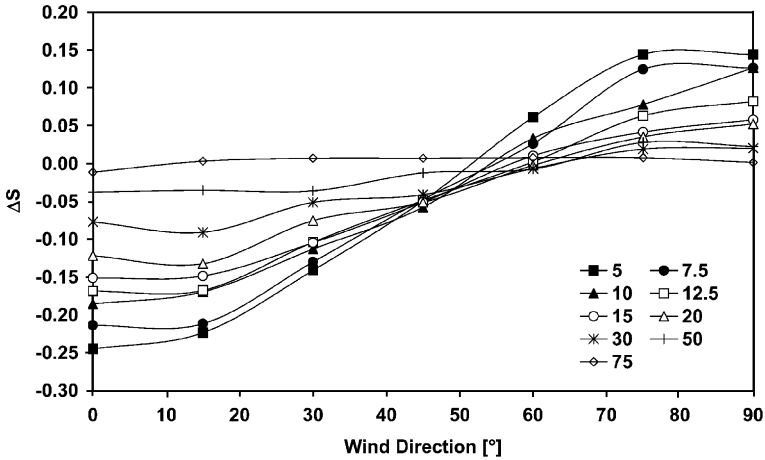


Fig. 13. Speed-up factor versus wind direction at base of circular hill. Heights from 5 to 75 mm above the surface are plotted. Measurement points is directly upwind of hill when wind is from 0°. Measurement point is beside hill when wind is from 90°.

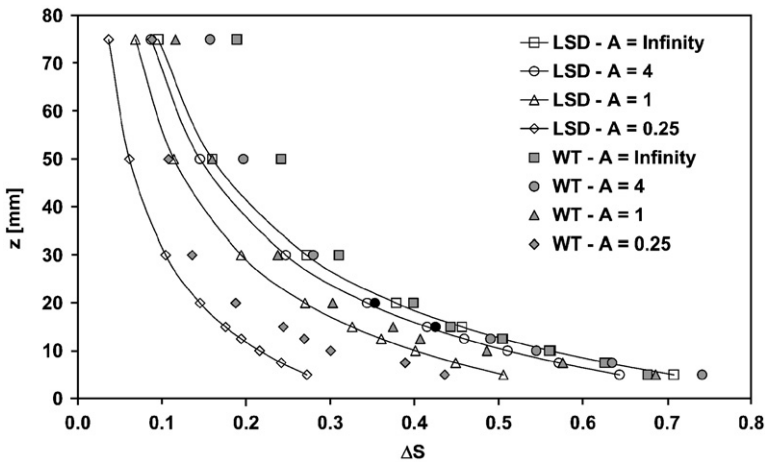


Fig. 14. Hilltop speed-up factor profiles for four hill aspect ratios:  $A = 0.25, 1, 4$  and  $\infty$ . WT denotes the present wind-tunnel measurements. Predictions of the LSD method are also shown.

### 2.9. Hill shoulder

It is interesting to note the variation in speed-up factor at the “shoulder” measurement locations as the aspect ratio is changed. The shoulder locations are those where  $x = 0$  with a 0° wind. Measurement points available included  $y = 0$  (the hill top) and  $y = L_2$  (the “shoulder face”). Wind-tunnel width limitations precluded taking base measurements ( $y = 2L_2$ ) for  $A = 4$ . It is apparent that the values of  $\Delta S$  peak for the circular hill ( $A = 1$ ),

Table 3

Measured values of  $\Delta S$  at the shoulder location ( $x = 0, y = L_2, \theta = 0^\circ$ ) at different heights above ground  $z$ , for hills of different aspect ratio  $A = L_2/L_1$

$z$ [mm]	$A = \infty$	$A = 4$	$A = 1$	$A = 0.25$	$A = 0$
5	0.677	0.487	0.532	0.249	-0.043
7.5	0.626	0.409	0.437	0.239	-0.027
10	0.560	0.331	0.360	0.174	-0.024
12.5	0.504	0.257	0.289	0.158	-0.018
15	0.443	0.210	0.250	0.150	-0.009
20	0.399	0.169	0.225	0.115	0.004
30	0.310	0.099	0.157	0.085	0.011
50	0.242	0.051	0.095	0.063	0.017
75	0.189	0.006	0.081	0.053	0.027

as shown in Table 3. This effect is believed to be due to lateral (“y direction”) acceleration of the flow horizontally on the windward face of the hill, in addition to the longitudinal (“x direction”) acceleration that is the primary cause of speed-up.

### 2.10. Analysis of prediction schemes

For the hilltop of the two-dimensional ridge, the existing speed-up prediction algorithms can be modified in a straight-forward manner to include wind direction effects. Similar to the Baker and FAA interpolation methods described earlier, it is also possible to fit simple cosine curves to describe wind direction variation

$$\Delta S(\theta) = \Delta S_0(0.5 + 0.5 \cos(2\theta)), \quad (6)$$

$$\Delta S(\theta) = \Delta S_0 \cos(\theta). \quad (7)$$

The Baker method (Eq. (4)), the FAA method and the two cosine fits were applied to the speed-up prediction algorithms for the top of the two-dimensional hill. Each of these methods fits a slightly different curve to the speed-up prediction. For example, Fig. 15 shows the hilltop  $\Delta S$  predicted at  $z = 10$  mm by applying each of the four wind direction methods to the results of the Weng non-linear prediction algorithm. It is readily apparent that the FAA method predicts higher speed-up than the others as  $\theta$  approaches  $90^\circ$ . It is not possible to say that one interpolation method performs better than the others, given the uncertainty level of the wind-tunnel measurements of  $\Delta S$ , and the difficulty of separating the wind direction interpolation from an overall speed-up prediction scheme.

### 3. Field comparisons: speed-up at Altamont pass

The accuracy of the available unmodified speed-up prediction schemes varies widely when used to predict the speed-up over actual hills. Weng et al. (2000) compare their Guidelines, as well as those of Taylor and Lee (1984) with field measurements from several sites. The accuracy of both methods depended most strongly on the site itself: for example, Askervein Hill (Taylor and Teunissen, 1987) predictions agreed well with actual measurements, while predictions for Nyland Hill (Mason, 1986) significantly

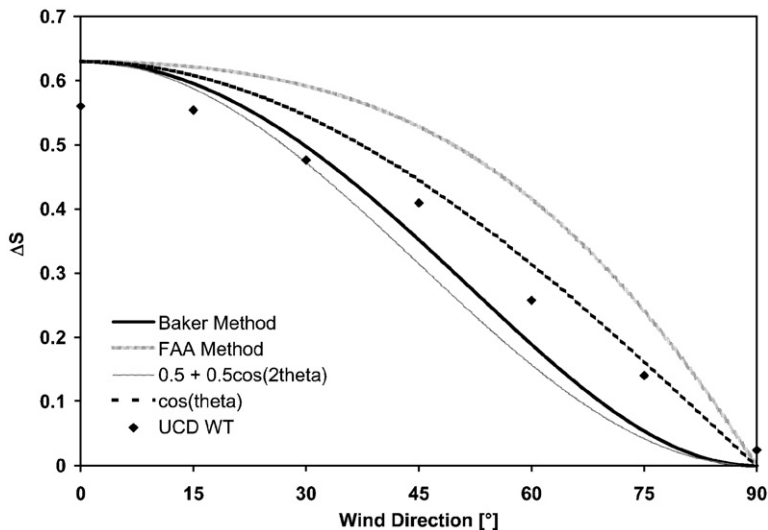


Fig. 15. Speed-up factors for the two-dimensional hill top at  $z = 10$  mm predicted by the non-linear Weng et al. formulation, using four different wind direction interpolation methods.

underestimated  $\Delta S$  at all heights. Geographic sensitivity is significant for all of the prediction schemes outlined above.

Since most of the field data used to evaluate the prediction schemes are from single hills surrounded by relatively flat terrain, it was desired to find the degree of accuracy that might be achieved at a complex terrain site. This was motivated by a desire to determine if the speed-up prediction schemes could be useful at wind energy generation sites. A ridge at Altamont Pass, California, USA was found where these methods could be applied directly to the un-modified prediction schemes. As shown in Fig. 16, a meteorological tower (“Tower A”) is situated on the crest of a ridgeline that is oriented approximately perpendicular to the prevailing summer wind direction of  $240^\circ$ . A fully instrumented meteorological tower operated by the Lawrence Livermore National Laboratory (LLNL) is situated on a bearing of  $240^\circ$  from the anemometer tower, about 4.5 km away in flat terrain, providing reference conditions for speed-up factor calculations.

The terrain between the LLNL tower and Tower A consists of mostly flat plain, followed by a steep uniform rise to the ridge crest location of Tower A (Fig. 17). The hill type is taken to be a two-dimensional ridge with  $h = 235$  m and  $L_1 = 503$  m. The land use is open grassland with  $z_0 = 15$  mm. Using these parameters, the prediction schemes were used to predict the speed-up at  $z = 24.4$  m (the height of the Tower A anemometer). The results are shown in Table 4. The variation in predicted  $\Delta S$  is typical of the amount of variation observed between the methods.

Calculation of the measured speed-up factor at a given time was complicated by the differing observation heights at the LLNL tower (10 and 40 m) and Tower A (24.4 m). A power law profile was fit to the LLNL 10 and 40 m wind speed readings and used to interpolate the LLNL wind speed at 24.4 m. The power-law relation was then used to calculate  $\Delta S$ . This method was used to generate a dataset of speed-up observations

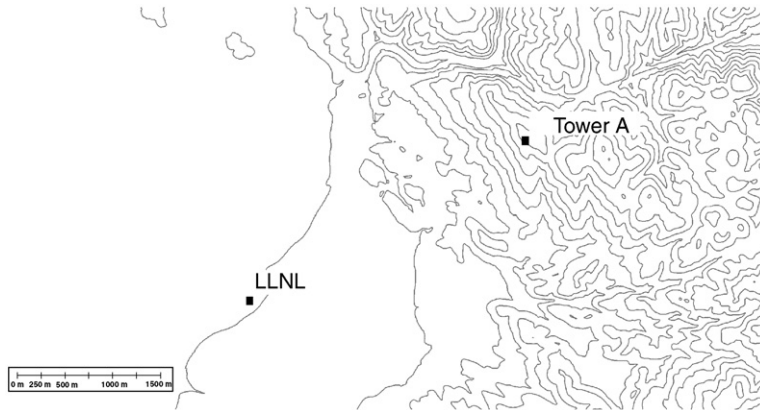


Fig. 16. Contour map of western side of Altamont Pass showing location of LLNL meteorological tower and Tower A. Contour interval 25 m. North is up.

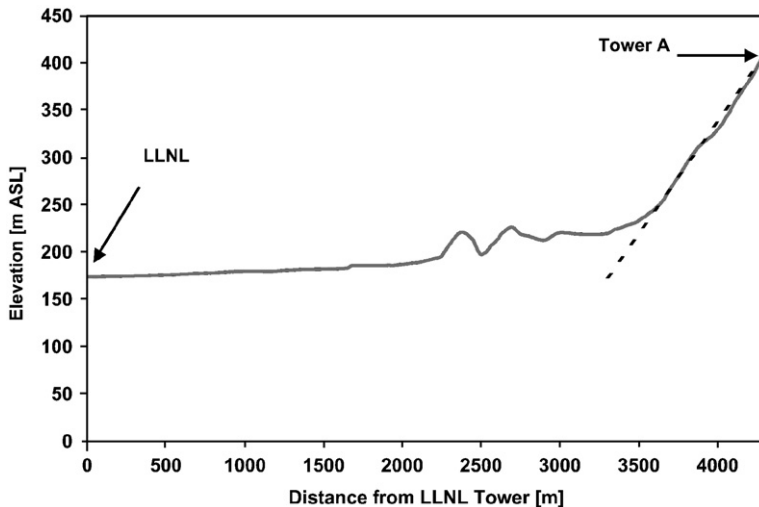


Fig. 17. Elevation transect from LLNL meteorological tower to Tower A. Dotted line shows hill slope approximation used for prediction schemes.

at Tower A on a half-hourly basis between 1 July 2001 and 30 June 2003. Observations when the wind direction was between  $235^\circ$  and  $245^\circ$  were used for comparison purposes.

All of the prediction schemes are limited to the case of a neutrally stable atmosphere. It has been observed that stability significantly impacts flow in the Altamont Pass. To control for this, the observations were binned by Pasquill-Gifford stability class (“A” = unstable, “C” = neutral, “F” = very stable). Table 5 shows the average speed-up factor calculated for Tower A, as well as the standard deviation, and the number of times each stability class was observed when winds were between  $235^\circ$  and  $245^\circ$ . The average speed-up under neutral (class “C”) conditions was  $\Delta S = 0.87$ , which is within the range of values in

Table 4

Speed-up factors predicted by various prediction schemes for Tower A relative to the LLNL tower, at a height of  $z = 24.4$  m above ground

Prediction method	$\Delta S$ at anemometer height
Eq. (2b)	0.935
FAA	0.808
Lemelin, Surry and Davenport	0.784
Taylor and Lee	0.808
Weng et al. (linear)	0.691
Weng et al. (non-linear)	0.620

Table 5

Observed  $\Delta S$  and standard deviation for each stability class at Tower A

Pasquill-Gifford stability class	$\Delta S$	Standard deviation	Number of observations
A	1.12	0.47	6
B	1.27	1.67	133
C	0.87	0.52	200
D	1.52	1.10	563
E	2.93	1.74	151
F	3.28	2.38	51
All	1.64	1.47	1104

Wind direction between  $235^\circ$  and  $245^\circ$ , 1 July 2001–30 June 2003.

**Table 4.** Interestingly, the least sophisticated methods (such as Eq. (2b)) gave the best predictions in this case.

Neutral conditions corresponded to a minimum speed-up. It is known that under stable conditions in this location, winds can be high aloft but are prevented from mixing down to the plains. Under unstable conditions, it is believed that additional heating of the terrain to the east of the Pass results in a relative increase in winds through the Pass. It should be noted that the standard deviation of  $\Delta S$  within a stability class remains high, suggesting that at any given time, there may be significant variation in actual conditions. This result suggests that the ability of the prediction schemes to accurately predict  $\Delta S$  at an arbitrary, specific time is less than ideal.

Defining the wind direction is somewhat problematic, since in reality it is possible for the wind direction at the one meteorological tower to be different from the direction at the second.  $\Delta S$  is dependent on which tower is used to define wind direction, and also the range of wind directions that are included in the average. Table 6 illustrates this feature by tabulating the  $\Delta S$  determined using increasingly wider wind direction ranges based on both the LLNL tower and Tower A.

By relaxing the requirement that the LLNL tower be upwind of Tower A to calculate  $\Delta S$ , the variation of  $\Delta S$  with respect to wind direction could be investigated. Results are shown in Fig. 18. The wind direction at Tower A was used as the representative wind direction in this case since at off angles the wind direction might vary appreciably in the plain, relative to a ridgetop location. As the wind vector is changed northward from  $240^\circ$  (which is taken as  $0^\circ$  relative wind direction),  $\Delta S$  decreases as the wind direction becomes

Table 6

Average  $\Delta S$  observed for different wind direction inclusion criteria, such as which location was used to measure the wind direction, and range of directions included

Wind direction range	Wind vane location	Average $\Delta S$		Number of observations	
		All data	Class C	All data	Class C
235–245	LLNL	1.64	0.87	1104	200
225–255	LLNL	1.58	0.89	3409	614
210–270	LLNL	1.52	0.85	6398	1169
235–245	Tower A	1.51	0.81	1463	315
225–255	Tower A	1.62	0.83	4803	991
210–270	Tower A	1.98	0.85	9214	1565

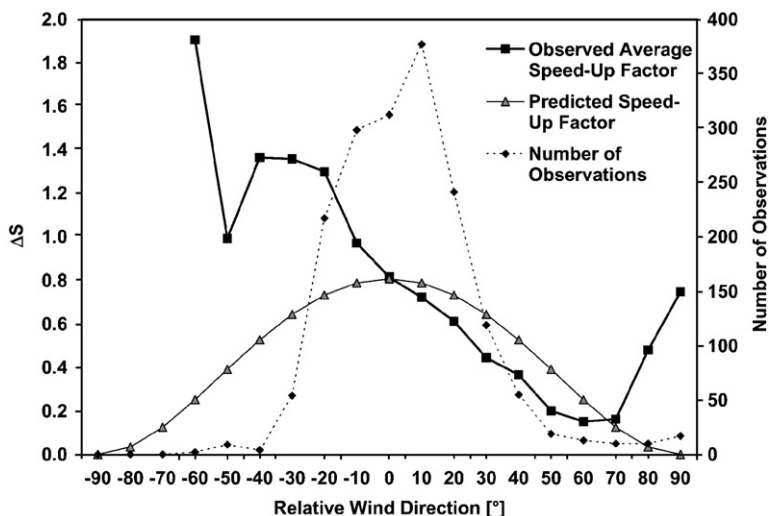


Fig. 18. Average speed-up factor at Tower A as a function of wind direction relative to perpendicular to the ridgeline. A wind from 240° is perpendicular to the ridgeline, and therefore corresponds to a relative wind direction of 0°. The number of observations included in each average is also shown. For comparison, results from the Taylor and Lee prediction scheme with a Baker wind direction modification are also presented.

more aligned with the ridgeline, up until a relative wind direction of about 60°. At angles greater than this, and also at negative relative wind directions,  $\Delta S$  increases where it perhaps would be expected to decrease. This could be due to a low number of observations, and the fact that the actual ridge is different from the idealized two-dimensional modeled ridge, especially to the southeast where ridgeline changes direction and increases in height.

Overall, the observed speed-up factors showed significant variability, even within the same stability class and wind direction range. One reason may be that stability class could be determined only from measurements at the Livermore tower: conditions at Tower A could still vary widely. Given the simplicity of the speed-up prediction schemes available, and the wide variability in observed speed-up ratios even under similar stability,

predicting wind conditions at a specific place and time using these methods may not be feasible if a large degree of accuracy is required. Further application of the un-modified prediction schemes to sites within the Altamont Pass was hampered by the lack of adjacent flat reference sites, and extremely complex terrain that made it difficult to estimate parameters such as  $h$  and  $L_1$ .

#### **4. Conclusions**

Wind-tunnel tests and field measurements were used to investigate how local wind direction impacts speed-up over hills. The wind-tunnel test results highlighted the limitations of current empirical speed-up prediction models. For the most part, current models are limited to simple hill geometries with shallow slopes and do not include the negative speed-up that occurs at the base of steep hills, effects of non-orthogonal wind directions or the local horizontal component of flow acceleration that occurs on the sides of hills with aspect ratios near one.

Wind-tunnel tests showed that the current models could be extended to include wind direction effects using simple interpolating factors. However, a comparison of speed-up predictions and actual measurements for a complex terrain site suggested that the significant variability often found in nature would be difficult to characterize using any empirical model based on only a few variables. While the speed-up prediction algorithms available are useful for estimating order of magnitude effects or maximum possible wind loads on a structure, they are inherently not sophisticated enough for applications in such fields as wind energy forecasting, that require an accurate prediction of the speed-up at specific times under a variety of atmospheric conditions. As such, current speed-up models have probably reached a level of sophistication appropriate for an empirical method based on a few, primarily geometric, variables.

#### **Acknowledgments**

The research documented here was performed as part of the California Regional Wind Energy Forecasting System Development initiative, a California Energy Commission (CEC) project managed by the Electric Power Research Institute (EPRI). Funding was provided by CEC through the Public Interest Energy Research (PIER) Program. The support of Dr. Charles McGowin of EPRI, and Dr. Dora Yen-Nakafuji of CEC is gratefully acknowledged. The authors also wish to thank Robert Szymanski of Powerworks, Inc.

#### **References**

- Baker, C., Wood, C., Gawthorpe, R., 1985. Strong winds in complicated hilly terrain—field measurements and wind-tunnel study. *J. Wind. Eng. Ind. Aerodynam.* 18, 1–26.
- Baker, C.J., 1985. The determination of topographical exposure factors for railway embankments. *J. Wind. Eng. Ind. Aerodynam.* 21, 89–99.
- Bowen, A., Lindley, D., 1977. A wind-tunnel investigation of the wind speed and turbulence characteristics close to the ground over various escarpment shapes. *Boundary-Layer Meteorol.* 12, 259–271.
- Carpenter, P., Locke, N., 1999. Investigation of wind speeds over multiple two-dimensional hills. *J. Wind Eng. Ind. Aerodynam.* 83, 109–120.

- Deaves, D., 1980. Computations of wind flow changes over two-dimensional hills and embankments. *J. Wind Eng. Ind. Aerodynam.* 6, 89–112.
- Derickson, R.G., Peterka, J.A., 2004. Development of a powerful hybrid tool for evaluating wind power in complex terrain: atmospheric numerical models and wind tunnels. In: *Proceedings of AIAA/ASME Wind Energy Symposium*, Reno, NV, USA, AIAA Paper No. 2004-1005.
- Engineering Sciences Data Unit, 1990. *Strong Winds in the Atmospheric Boundary Layer Part 1: Mean-Hourly Wind Speeds*. ESDU Publication 82026.
- Federal Aviation Administration, 1988. *Siting Guidelines for Low Level Wind Shear Alert System (LLWAS) Remote Facilities*. FAA Publication 6560.21.
- Finnigan, J.J., 1988. Air flow over complex terrain. In: Steffen, W.L., Denmead, O.T. (Eds.), *Flow and Transport in the Natural Environment: Advances and Applications*. Springer, Berlin, pp. 183–299.
- Gong, W., Ibbetson, A., 1989. A wind tunnel study of turbulent flow over model hills. *Boundary-Layer Meteorol.* 49, 113–148.
- Hunt, J.C.R., Leibovich, S., Richards, K.J., 1988. Turbulent shear flow over low hills. *Q. J. Roy. Meteorol. Soc.* 114, 1435–1470.
- Jackson, P.S., 1979. The influence of local terrain features on the site selection for wind energy generating systems. *Boundary Layer Wind Tunnel Laboratory Internal Report*, University of Western Ontario, BLWT-1-1979.
- Jackson, P.S., Hunt, J.C.R., 1975. Turbulent wind flow over a low hill. *Q. J. Roy. Meteorol. Soc.* 101, 929–955.
- Kaimal, J., Finnigan, J., 1994. *Atmospheric Boundary Layer Flows—Their Structure and Measurement*. Oxford University Press, Oxford.
- Kim, H.G., Lee, C.M., Lim, H.C., Kyong, N.H., 1997. An experimental and numerical study on the flow over two-dimensional hills. *J. Wind Eng. Ind. Aerodynam.* 66, 17–33.
- Kim, H.G., Patel, V.C., Lee, C.M., 2000. Numerical simulation of wind flow over hilly terrain. *J. Wind Eng. Ind. Aerodynam.* 87, 45–60.
- Lemelin, D., Surry, D., Davenport, A., 1988. Simple approximations for wind speed-up over hills. *J. Wind Eng. Ind. Aerodynam.* 28, 117–127.
- Lindley, D., Neal, D., Pearse, J.R., Stevenson, D.C., 1981. The effects of terrain and construction method on the flow over complex terrain models in a simulated atmospheric boundary layer. In: *Proceedings of the Third British Wind Energy Association Wind Energy Conference*, Cranfield, UK, pp. 195–211.
- Mason, P., Sykes, R., 1979. Flow over an isolated hill of moderate slope. *Q. J. Roy. Meteorol. Soc.* 105, 383–395.
- Mason, P.J., 1986. Flow over the summit of an isolated hill. *Boundary-Layer Meteorol.* 37, 385–405.
- Miller, C.A., Davenport, A.G., 1998. Guidelines for the calculation of wind speed-ups in complex terrain. *J. Wind Eng. Ind. Aerodynam.* 74–76, 189–197.
- Ohba, R., Hara, T., Nakamura, S., Ohya, Y., Uchida, T., 2002. Gas diffusion over an isolated hill under neutral, stable and unstable conditions. *Atmospheric Environment* 36, 5697–5707.
- Snyder, W.H., 1981. *Guideline for fluid modeling of atmospheric diffusion*. EPA-600/8-81-009. United States Environmental Protection Agency.
- Taylor, P.A., 1998. Turbulent boundary-layer flow over low and moderate slope hills. *J. Wind Eng. Ind. Aerodynam.* 74–76, 25–47.
- Taylor, P.A., Lee, R.J., 1984. Simple guidelines for estimating wind speed variations due to small scale topographic features. *Climatol. Bull.* 18 (2), 3–22.
- Taylor, P.A., Teunissen, H.W., 1987. The Askervein Hill project: overview and background data. *Boundary-Layer Meteorol.* 39, 15–39.
- Weng, W., Taylor, P.A., Walmsley, J.L., 2000. Guidelines for airflow over complex terrain: model developments. *J. Wind Eng. Ind. Aerodynam.*